

## 1. Calculation Methods

In one method, the electron transfer number ( $n$ ) of the ORR process were calculated by the Koutecky-Levich (K-L) equation:

$$J^{-1} = J_k^{-1} + (B\omega^2)^{-1}$$
$$B = 0.2 \times n \times F \times C_{O_2} \times D_{O_2}^{\frac{2}{3}} \times \nu^{-\frac{1}{6}}$$

where  $J$  is the measured current density during ORR,  $J_k$  is the kinetic current density,  $\omega$  is the electrode rotating angular velocity ( $\omega = 2\pi N$ ,  $N$  is the linear rotation speed),  $B$  is the slope of K-L plots,  $n$  represents the electron transfer number,  $F$  is the Faraday constant ( $F = 96485 \text{ C mol}^{-1}$ ),  $D_0$  is the diffusion coefficient of  $O_2$  in 0.1 M KOH ( $1.9 \times 10^{-5} \text{ cm}^2 \text{ s}^{-1}$ ),  $\nu$  is the kinetic viscosity ( $0.01 \text{ cm}^2 \text{ s}^{-1}$ ),  $C_0$  is the bulk concentration of  $O_2$  ( $1.2 \times 10^{-3} \text{ mol L}^{-1}$ ).

In another method, the electron transfer number ( $n$ ) and peroxide yield were quantified by the RRDE measurements. The ring potential was set constantly at 1.55 V vs. RHE. The peroxide yield ( $H_2O_2$  %) and electron transfer number ( $n$ ) were determined by the followed equations

$$n = 4 \times \frac{I_d}{I_d + \frac{I_r}{N}}$$
$$H_2O_2\% = \frac{200 \times \frac{i_r}{N}}{i_d + \frac{i_r}{N}}$$

Where  $i_d$  and  $i_r$  stand for the disk and ring current, respectively, and  $N$  is the current collection efficiency (0.37) of the Pt ring of the RRDE electrode.

## 2. Test method of zinc-air battery

First, 0.01 g catalyst was suspended in 0.74 mL purified water, 0.2 mL isopropanol, and 60  $\mu\text{L}$  5 wt% Nafion solution to produce catalyst ink. Then, the air-cathode was fabricated via dropping 100  $\mu\text{L}$  catalyst ink onto  $1 \text{ cm}^{-2}$  hydrophobic carbon cloth. Thus, the catalyst loading is  $\sim 0.001 \text{ g cm}^{-2}$ . Combined with the Zn-foil anode and 6 M KOH/0.2 M  $(\text{CH}_3\text{COO})_2\text{Zn}$  electrolyte, the liquid ZABs can be obtained. Discharge and charge performance of liquid ZAB was test by LSV

technique at a scan rate of  $10 \text{ mV s}^{-1}$  on a Chenhua CHI 660E electrochemical work station in ambient atmosphere. The galvanostatic discharge and charge-discharge cycling (10 min charge and 10 min discharge) were recorded by using a LAND testing system at a current density of  $10 \text{ mA cm}^{-2}$ . The specific capacity and the energy density were calculated normalized to the mass of the consumed zinc according the following equations:

$$\text{Specific capacit} = \frac{\text{Current} \times \text{Discharge time}}{\text{Weight of consumed Zn}}$$

$$\text{Energy density} = \frac{\text{Current} \times \text{Discharge time} \times \text{Average discharge voltage}}{\text{Weight of consumed Zn}}$$

### 3. Supplementary Figures and Tables

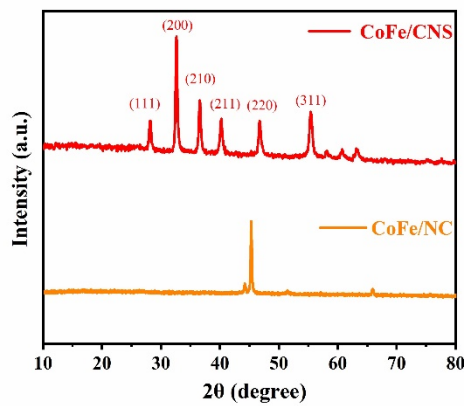


**Figure S1.** the XRD of  $(\text{Co,Fe})\text{S}_2/\text{CNS}$  and  $\text{CoFe/CN}$

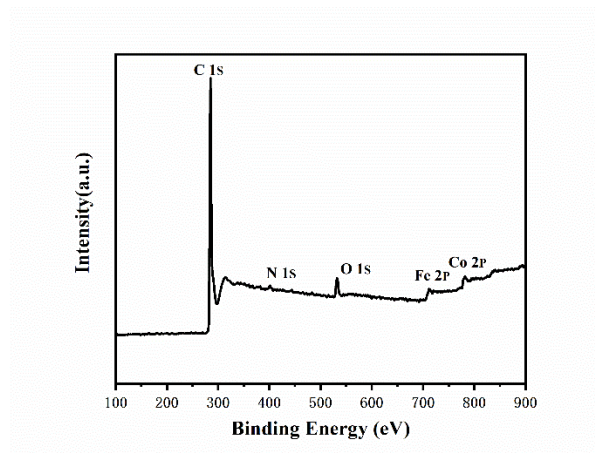


**Figure S2.** XPS survey spectrum of  $\text{CoFe/CN}$

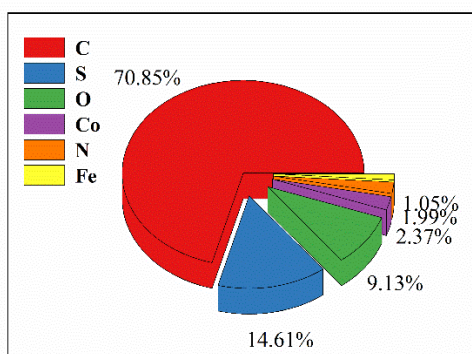


**Figure S3.** Elemental analysis of (Co,Fe)S<sub>2</sub>/CNS by xps

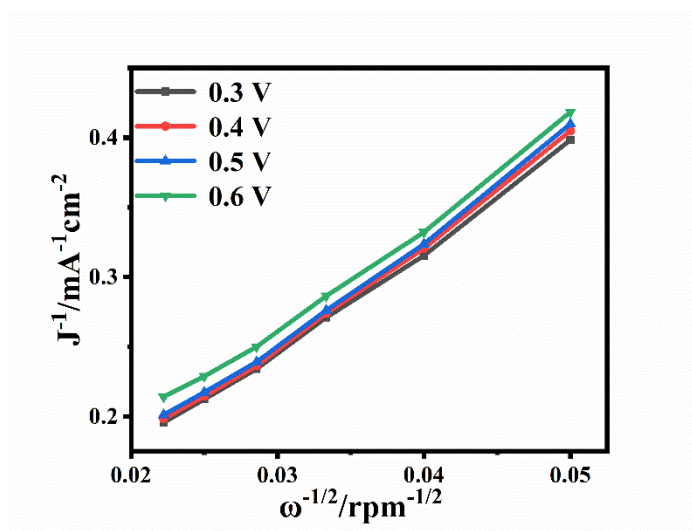


**Figure S4.** K-L plots of (Co,Fe)S<sub>2</sub>/CNS at different potentials

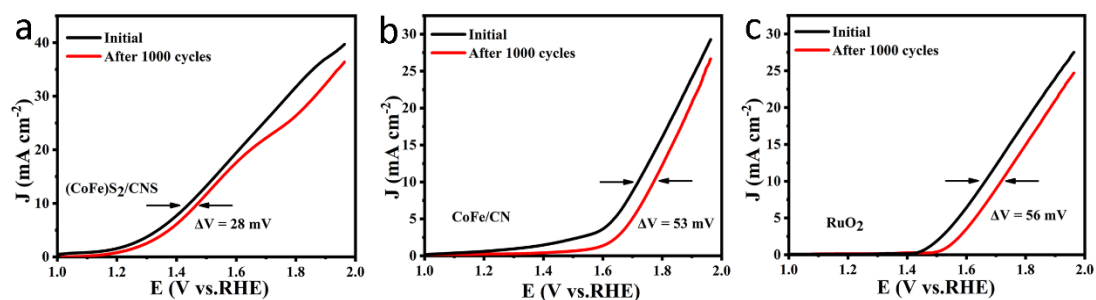


**Figure S5** Polarization curves of the (a) (Co,Fe)S<sub>2</sub>/CNS catalyst, (b) CoFe/CN catalyst, and (c) commercial RuO<sub>2</sub> catalysts before and after 1000 cycles in 0.1 M KOH solution.

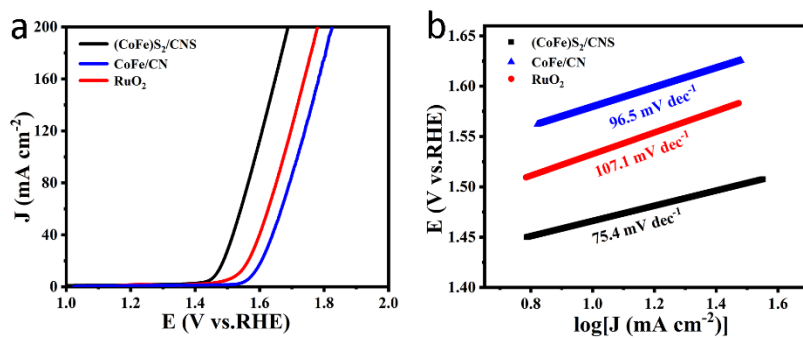


**Figure S6** (a) LSV curves for the OER of the  $(\text{Co,Fe})\text{S}_2/\text{CNS}$ ,  $\text{CoFe}/\text{CN}$ , and  $\text{RuO}_2$  catalysts in 1 M KOH; (b) The corresponding Tafel plots.

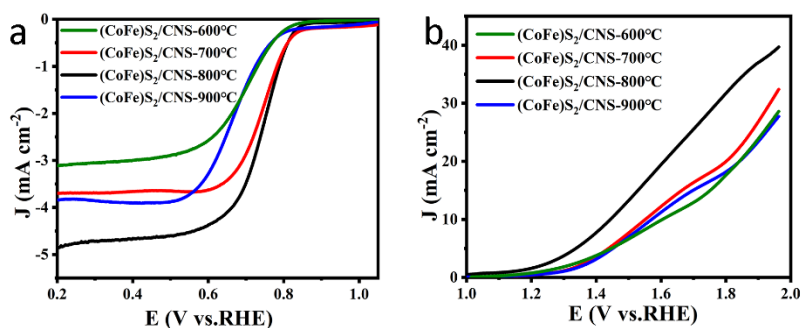


**Figure S7** (a-b)  $(\text{Co,Fe})\text{S}_2/\text{CNS}$  catalyst was cured at  $600^\circ\text{C}$ ,  $700^\circ\text{C}$ ,  $800^\circ\text{C}$ , and  $900^\circ\text{C}$  with ORR and OER.

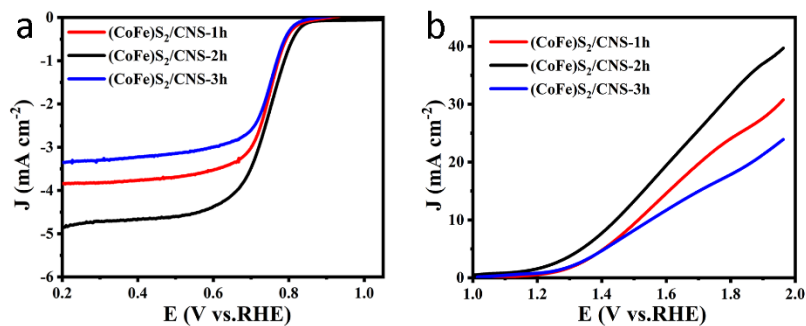


**Figure S8** (a-b) Curing time is 1h, 2h and 3h at  $800^\circ\text{C}$ , respectively. ORR and OER of  $(\text{Co,Fe})\text{S}_2/\text{CNS}$  catalyst.

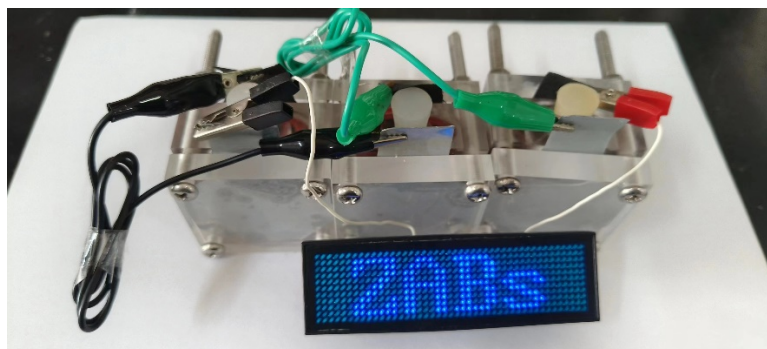


**Figure S9.** An LED display lighted by three Zn–air batteries connected in series.

**Table S1.** List of the ORR/OER catalytic properties of the (Co,Fe) $S_2$ /CNS and previously reported state-of-the-art catalysts in 0.1 M KOH.

Catalyst	Electrolyte	ORR	ORR	OER	OER	E=E(j=10)	Ref
		$E_{onset}/$ V(vs RHE)	$E_{1/2}/V$ (vs RHE)	$E_{onset}/$ V(vs RHE)	$E_{(j=10)}/$ V(vs RHE)	$E_{1/2}/V$ (vs RHE)	
(Co,Fe) $S_2$ /CNS	0.1 MKOH	0.84	0.74	1.30	1.42	0.68	Our work
(Ni,Co) $S_2$	0.1 MKOH	0.82	0.71	1.47	1.50	0.79	1
CoFe/N-GCT	0.1 MKOH	0.94	0.70	1.51	1.64	0.88	2
Co $_3$ FeS $_{1.5}$ (OH) $_6$	0.1 MKOH	0.87	0.72	N.A.	1.59	0.87	3
Co-Ni-S@NSP	0.1 MKOH	0.95	0.82	1.57	1.7	0.88	4
Fe@C- NG/NCNTs	0.1 MKOH	N.A.	0.84	N.A.	1.62	0.84	5
N-CoS $_2$ YSSs	1 M KOH	0.95	0.81	1.50	1.52	0.71	6

**Table S2.** Comparative summary of the energy efficiency of currently available ZABs with our work.

Electrocatalysts	Electrolytes	OCP (V)	Power density (mW cm <sup>-2</sup> )	Specific capacity (mAh g <sup>-1</sup> )	Cyclic stability	Ref
(Co,Fe)S <sub>2</sub> /CNS	6 M KOH+0.2 M Zn <sup>2+</sup>	1.453 V	115	759.1	360 cycles(120h)	Our work
Co-N,B-CSs	6 M KOH+0.2 M Zn <sup>2+</sup>	1.49	103	403	40 cycles (15 h)	7
FeCo@MNC	6 M KOH+0.2 M Zn <sup>2+</sup>	1.41	115	N.A.	144 cycles (24 h)	8
Co <sub>9</sub> S <sub>8</sub> /CNT	6 M KOH+0.2 M Zn <sup>2+</sup>	1.43	197.6	N.A.	576 cycles (96 h)	9
S-GNS/NiCo <sub>2</sub> S <sub>4</sub>	6 M KOH+0.2 M Zn <sup>2+</sup>	N.A.	188.6	N.A.	150 cycles (100 h)	10
Co/N-CNSNs	6 M KOH+0.2 M Zn <sup>2+</sup>	1.471	81.7	638.4	100 cycles (100 h)	11
Co <sub>3</sub> FeS <sub>1.5</sub> (OH)	6 M KOH+0.2 M Zn <sup>2+</sup>	N.A.	113.12	898	108 cycles (36 h)	3
FeCo/FeCoNi@NCNTs-HF	6 M KOH+0.2 M Zn <sup>2+</sup>	1.469	156.2	783	180 cycles (120 h)	12
Fe-SAs/NPS-HC	6 M KOH+0.2 M Zn <sup>2+</sup>	1.45	195.0	N.A.	500 cycles (200,000 s)	13

## References

1. J. Zhang, X. Bai, T. Wang, W. Xiao, P. Xi, J. Wang, D. Gao and J. Wang, *Nano-Micro Letters*, 2019, **11**, 2.
2. X. Liu, L. Wang, P. Yu, C. Tian, F. Sun, J. Ma, W. Li and H. Fu, *Angewandte Chemie International Edition*, 2018, **57**, 16166-16170.
3. H.-F. Wang, C. Tang, B. Wang, B.-Q. Li and Q. Zhang, *Advanced Materials*, 2017, **29**, 1702327.
4. W. Fang, H. Hu, T. Jiang, G. Li and M. Wu, *Carbon*, 2019, **146**, 476-485.
5. Q. Wang, Y. Lei, Z. Chen, N. Wu, Y. Wang, B. Wang and Y. Wang, *Journal of Materials Chemistry A*, 2018, **6**, 516-526.
6. X. F. Lu, S. L. Zhang, E. Shangguan, P. Zhang, S. Gao and X. W. Lou, *Advanced Science*, 2020, **7**, 2001178.
7. Y. Guo, P. Yuan, J. Zhang, Y. Hu, I. S. Amiin, X. Wang, J. Zhou, H. Xia, Z. Song, Q. Xu and S. Mu, *ACS Nano*, 2018, **12**, 1894-1901.
8. C. Li, M. Wu and R. Liu, *Applied Catalysis B: Environmental*, 2019, **244**, 150-158.
9. H. Li, Z. Guo and X. Wang, *Journal of Materials Chemistry A*, 2017, **5**, 21353-21361.
10. W. Liu, J. Zhang, Z. Bai, G. Jiang, M. Li, K. Feng, L. Yang, Y. Ding, T. Yu, Z. Chen and A. Yu, *Advanced Functional Materials*, 2018, **28**, 1706675.
11. X. Huang, Y. Zhang, H. Shen, W. Li, T. Shen, Z. Ali, T. Tang, S. Guo, Q. Sun and Y. Hou, *ACS Energy Letters*, 2018, **3**, 2914-2920.
12. Z. Wang, J. Ang, B. Zhang, Y. Zhang, X. Y. D. Ma, T. Yan, J. Liu, B. Che, Y. Huang and X. Lu, *Applied Catalysis B: Environmental*, 2019, **254**, 26-36.
13. Y. Chen, S. Ji, S. Zhao, W. Chen, J. Dong, W.-C. Cheong, R. Shen, X. Wen, L. Zheng, A. I. Rykov, S. Cai, H. Tang, Z. Zhuang, C. Chen, Q. Peng, D. Wang and Y. Li, *Nature Communications*, 2018, **9**, 5422.